



Prediction model of limestone rock mass quality, using seismic wave velocity (Case study: Sarvak formation in Bakhtiari dam site)

Mehdi Kianpour, Seyed Mahmoud Fatemi Aghda*, Mehdi Talkhablou

Faculty of Earth Science, Kharazmi University, Tehran, Iran

Received 11 March 2018; accepted 16 December 2018

Abstract

The purpose of this study was to develop a model for the estimation of rock mass classification of Sarvak limestone in the Bakhtiari dam site, south-west (SW) Iran. Q system had been used as the starting point for the rock mass classification. This method was modified for sedimentary rock mass which is known as Q_{srm} . Because Q_{srm} considers a wide range of rock mass properties, it has become a tool for rock mass classification that more correlates with geophysical parameters. This study tried to revise and empower the correlation between P-wave velocity (V_p) with Q and Q_{srm} in Sarvak limestone. By using data sets of Bakhtiari Dam Site (BDS) in SW Iran and multivariate regression and the Fuzzy Inference System (FIS), models were rendered for prediction of Q and Q_{srm} . About 700 sets of data were used for modeling and V_p was considered as the input parameter. The regression equations showed the relationship between V_p with Q and Q_{srm} , under conditions of quadratic relations, obtained coefficients of determination (R^2) of 0.49 and 0.66, respectively. The correlation coefficient was calculated as 0.82 for the Q_{srm} obtained from FIS models. Also, Variance Accounted For (VAF) and Root Means Square Error (RMSE) indexes were also used for evaluation of prediction accuracy of models. Results showed that V_p has better performance in prediction of Q_{srm} than Q and the FIS model showed the best prediction results. Because these models have accuracy, they could be used in similar conditions.

Keywords: Rock Mass Quality, Sarvak Limestone, P-Wave Velocity, Empirical Equations, Fuzzy Inference System

1. Introduction

Numerous researchers have developed rock mass classification systems. One of the first such systems is Rock Quality Designation (RQD) (Deere 1963). The system accounts only for the frequency of joints within a rock mass. Later systems, such as Rock Mass Rating (RMR, Bieniawski 1973) and Q systems (Barton et al. 1974), use RQD as one of their measurable parameters, but also include factors such as intact rock strength, joint spacing, joint condition, field stress, number of joint sets and the effects of groundwater. GSI (Hoek 1994; Hoek et al. 1995; Hoek and Brown 1997; Marinos and Hoek 2001) method is based on an assessment of the lithology, structure, and condition of discontinuity surfaces in the rock mass and is estimated from visual examination of the rock mass exposed.

There is also, modified rock mass classification for sedimentary rock mass (Q_{srm}) that takes account of the geometry of rock mass, bedding, the nature of the lithotype and their structure and texture (Equation 1, Carozzo et al. 2008).

$$Q_{SRM} = RQD/J_n \times J_r/J_a \times J_w/SRF \times R_s/S \times T/V \quad (1)$$

In comparison to Q, Equation 1 has four further factors; R_s is the rating for the bedding, S is the rating for dipping of the layers, T is the rating for the texture of the rock mass and V is the rating for the presence of cavities. Characterization of a rock mass may also use information from geophysical methods, as described in numerous studies.

*Corresponding author.

E-mail address (es): d.kharazmi95@gmail.com

Barton (1991) proposed a basic model for the study of the relationship between the P-wave velocity and the Q value. This model was changed later for seismic analysis in other regions (Barton 1995, 2002, 2007). Also, many other studies for correlation between the rock mass quality and geophysical analysis were researched by others (e.g., Leucci and Giorgi 2006; Cardarelli et al. 2006).

Cha et al. (2006) and Zafirovski et al. (2012) investigated the relationship between the rock mass classification and the pressure and shear wave velocity near the earth's surface. Moreover, Bery and Saad (2012) found a relation using linear regression.

Bery and Rosli (2012) provided links between the engineering properties of calcareous rock masses and V_p in underground excavations. Azwinl et al. (2015) used V_p and electrical resistivity to estimate the geotechnical properties of rock masses. Krau et al. (2014) researched on the seismic travel-time and attenuation tomography to characterize the excavation damaged zones. Carozzo et al. (2008) conducted research on the pre-existing relationships between V_p and rock mass indexes (Q and Q_{srm}). This research can be considered as the most important research in predicting the Q_{srm} of limestone rock masses using geophysical methods. Later in the same research (Leucci and Giorgi 2015), the relationship between limestone rock mass quality and geophysical parameters based on the Q_{srm} classification was investigated.

Cao et al. (2015) show that V_p can be a promising tool to continuously monitor the relatively weak zone or

evaluate seismic hazard in underground coal mining. Hemmati-Nourani et al. (2017) used the V_p to estimate Q, RMR, and RQD of iron ore. In the study, there was a good relationship between V_p and rock mass quality indices. Fan et al. (2018) present an investigation of V_p transmission in complex rock masses; the rocks have different wave impedances on either side of a joint. Two cases, “soft-to-hard” and “hard-to-soft” rock masses, were used to demonstrate wave propagation through the complex rock masses.

The objective of this study was to determine the correlation between V_p with rock mass quality of Sarvak limestone in the Bakhtiari Dam Site (BDS). Sedimentary rocks present specific features such as layers and grain size, which must not be neglected in the characterization of rock quality. Also, the Q_{stm} classification system was not calculated and researched in geological formations of Iran so far.

2. Geological background of the study area

The study area was BDS located on the Bakhtiari river, 120 km away from the north of the Andimeshk city, SW of Khoramabad, Lorestan Province, Iran. According to the interpretation of surface geology and data of drilling and exploration boreholes, the dam site and its surrounding consist of folded carbonate sedimentary rocks that belong to Sarvak formation from the

Bangestan group. The Sarvak formation in BDS is divided into six units from SV1 (oldest) to SV6 (youngest). Generally, SV1 is marly limestone (gray color) with intercalations of marl and shale. SV2 is alternating layers of dark gray marly limestone and siliceous limestone. SV3 is similar to part SV2 with a large number of discontinuities that lead to changes in some parameters and the disturbed section has medium to thickly layered limestone. SV4 is thick to very thick gray, nodular limestone with silica nodules and rarely made of chert. SV5 had medium to thickest dark gray limestone and marly limestone with intercalations and in SV6, thin to the medium layers of dark gray to black limestone (0.2 to 0.4m) (Iran Water and Power resources development Co (IWPC) 2008). In Figure 1, the location and the geological map of BDS are shown. Also, a Joint study in all parts of the rock mass shows that the main discontinuities in the BDS consist of three sets of discontinuities (J_1 , J_2 , and J_3), bedding, and also random joints (faults and fractures). Structurally, two anticlines (Giriveh and SiahKuh) and three faults (F1, F2, and F3 fault) were seen in the studied area. Characteristics of discontinuities had been studied during the drilling of the tunnels (underground). The schematic 3D presentation of the discontinuities in the project area is shown in Figure 2 (IWPC 2007).

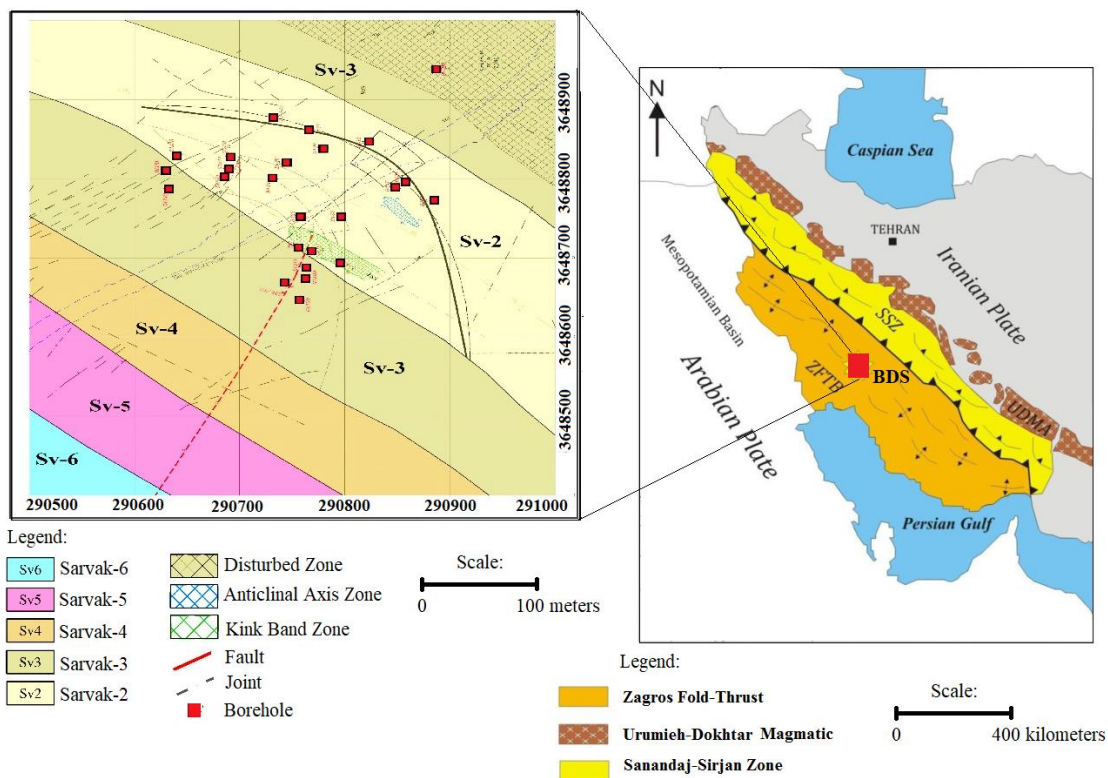


Fig 1. Geological map and the longitudinal geological section of BDS.

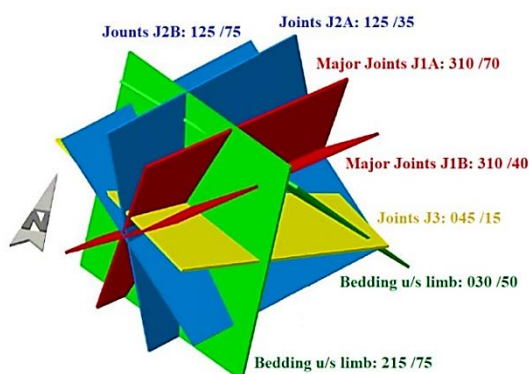


Fig 2. Schematic 3D presentation of the discontinuities in the project area.

3. Materials and Methods

In this study, for acquiring geophysical and geotechnical data, three-dimensional raster layers of V_p , Q , and Q_{srm} sections were prepared by interpolation methods between data-points, extracted from galleries and boreholes, in ArcGIS 10.3.1 software package. All data sets taken from galleries and drilled boreholes in the BDS, located in SW Iran. By using regression analyses and FIS methods, models are rendered for prediction of

Q and Q_{srm} in Sarvak limestone. About 700 sets of data have been used for modeling, and V_p was considered as the input parameter. The general principles underlying methods are shown in Figure 3. The results of FIS and regression analyses show that V_p in cases where there is no possibility of geotechnical study can predict limestone rock mass quality and stability parameters that have a remarkable effect on the Q_{srm} value. The results obtained are applied to any area with a similar geological formation, but a similar procedure may be applicable in other areas as well.

In BDS, geophysical investigations had been carried out by performing seismic tomography between different galleries at the right and left abutment. The purpose of the tomography survey was to assess the quality of rock mass at the valley of the dam site and to investigate the presence of probable weak zones. The tomography scan, in the left and right abutment, was performed by cross-gallery (or cross-borehole) arrangement in the foundation with source/receiver spacing of 2 m and source of explosive. Figure 4, shows galleries and studied boreholes between them and Figure 5 shows the geological section of galleries (IWPC 2007).

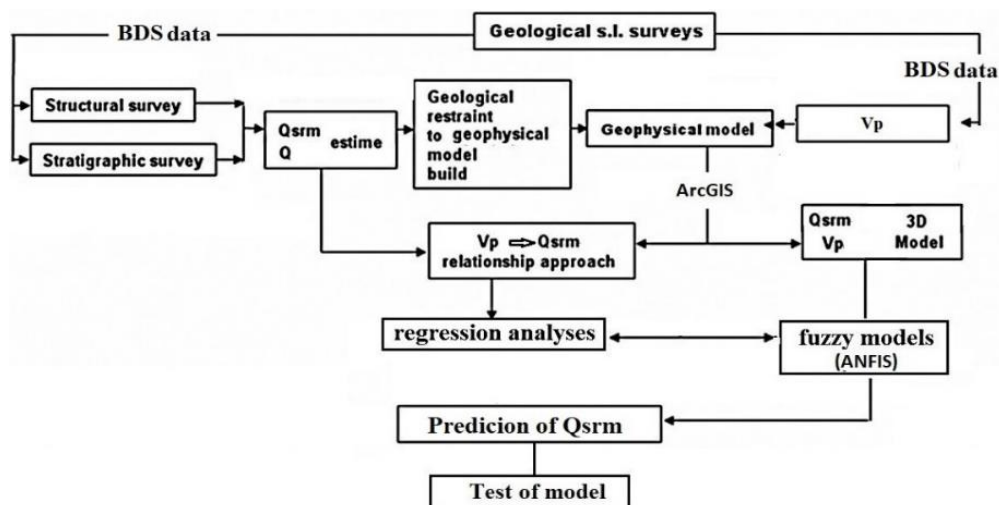


Fig 3. Flowchart of methods, used in this research, to evaluate rock mass quality.

The geophysical operation was done between the GL_1 - GL_2 , GL_2 - GL_3 , GL_7 - GL_{32} and GR_1 - GR_3 galleries and rock mass quality was calculated in galleries and all boreholes (SABIR Co 2004). For applying Q and Q_{srm} classification systems on the rock mass classes in BDS, a site visit was arranged, and Q and Q_{srm} classification systems were used for classifying the drill cores of several selected boreholes and galleries, drilled in different rock units from SV_1 (oldest) to SV_6 (youngest). Also, the results of the preliminary Q -classification were presented in Barton's site visit report for BDS (Barton

2008), but Q_{srm} was not calculated in BDS and other projects in Iran. Thus, in this research, Q and Q_{srm} indexes were calculated in GL_1 , GL_2 , GL_3 , GL_7 , GL_{32} , GR_1 and GR_3 galleries and in boreholes were drilled between them. Concerning Table 1 and Figure 6, Q values confirm the very poor to good quality and Q_{srm} values confirm the very poor to the fair quality of the BDS rock mass.

In the left abutment of BDS, the structural situation is similar to the right side, but the extension of the Kink Band Zone is reduced.

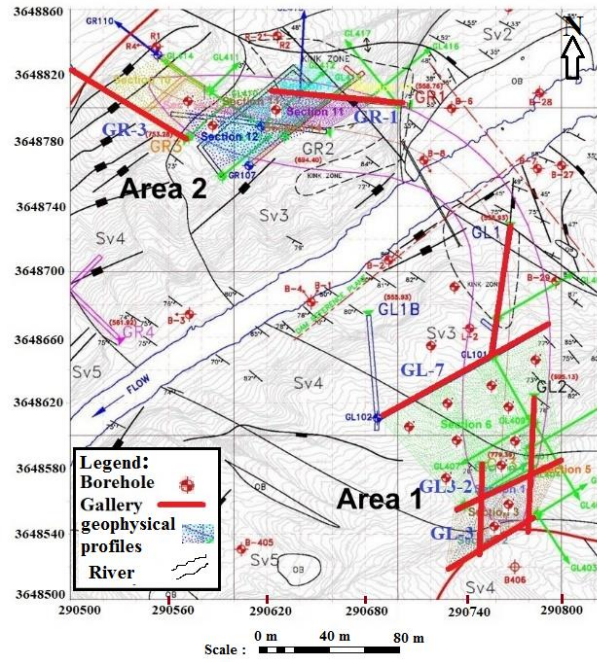


Fig 4. Studded galleries and boreholes in left (area 2) and right (area 1) abutments of BDS for seismic analyses and rock mass classification.

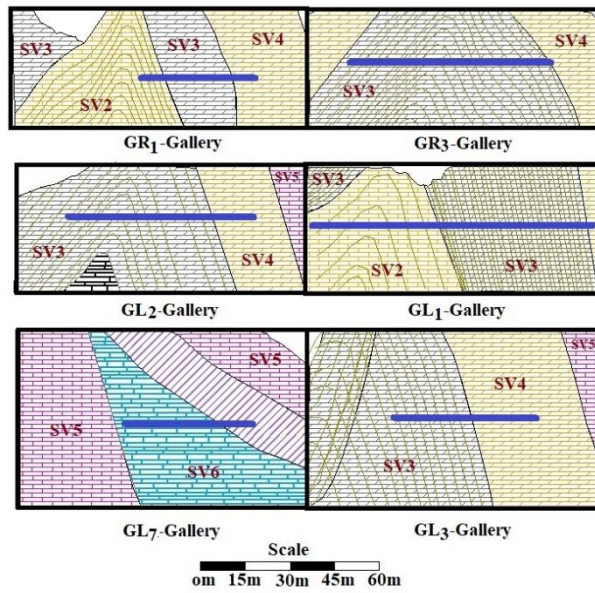


Fig 5. Geological section of GR₁, GR₃, GL₁, GL₂, GL₇ and GL₃ galleries in BDS.

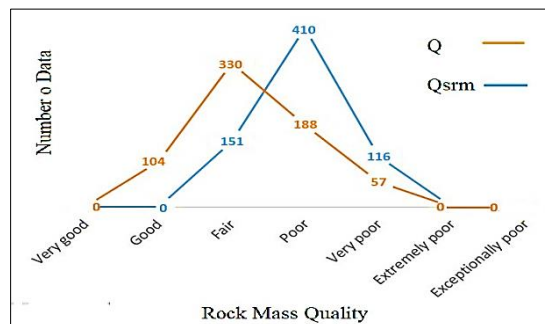


Fig 6. Generally, Q and Q_{srm} rock masses quality of BDS that show the number of data with very good to exceptionally poor quality.

In addition to open joints, also open bedding planes can be observed; these structures generally dip toward downstream, as they are located on the downstream side of the anticlinal axial plane. These structures have an effect on Q and Q_{srm} values.

To obtain the information layers of Q and Q_{srm} , first, throughout all the galleries and boreholes between them, the values of Q and Q_{srm} were calculated. Then, using the interpolation methods in the GIS software, the corresponding information layers were created that have an appropriate overlap in the points without the

measured data. Since the Q and Q_{srm} indices have been measured in all galleries and seismic tomography operations have also been performed between them, so the information layers of V_p , Q and Q_{srm} are completely consistent with each other and it is possible to extract data-sets from these layers at any point. Figure 7, shows ArcGIS raster layers of V_p , Q, and Q_{srm} .

3.1. Correlation between Q, Q_{srm} and V_p

A detailed comparison of the tomography sections with the corresponding rock mass quality maps (at the same scale) was performed.

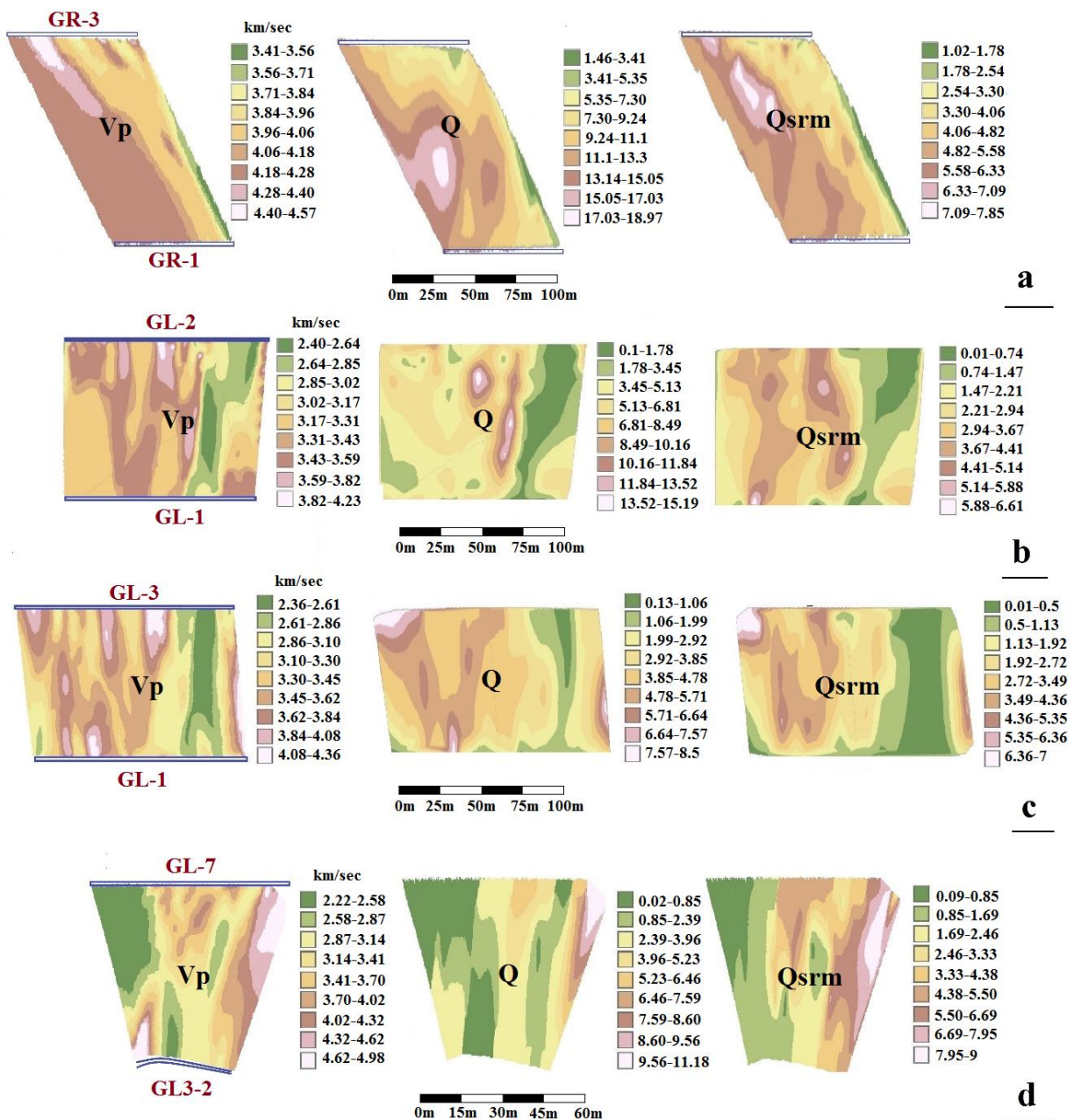


Fig 7. Modeling of geophysical (V_p) and rock mass quality (Q and Q_{srm}) raster layers by interpolation between data-sets in ArcGIS 10.3.1 software package (a-d).

Table 1. Generally, Q and Q_{srn} rock masses quality and relative parameters

Description	Exceptionally poor	Extremely poor	Very poor	Poor	Fair	Good	Very good
Q	0.001-0.01	0.01-0.1	0.01-1	1-4	4-10	10-40	40-100
Number off data	0	0	57	188	330	104	0
Q _{srn}	<0.0001	0.0001-0.01	0.01-1	1-4	4-100	100-400	400-1000
Number off data	0	0	116	410	151	0	0
Parameter	R _s	SRF	J _w	J _a	J _r	J _n	RQD%
Range	0.5-1	1-10	0.2-1	0.5-8	0.5-2	9-15	25-85

The results of reprocessed seismic tomography sections show a quite complex velocity field. The assessment and reprocessing study verified that the range of V_p is between 2.02 km/s and 4.08 km/s. As shown in Figure 7, in the left bank, between GL₁-GL₂ and GL₂-GL₃, briefly show the correlation between V_p and rock mass quality is possible. The best possible can be assumed in the profile between GL₃ and GL₂. The result of the GR₁-GR₃ seismic profile is interesting. Note that in the area closest to weak rocks or faulted zone, the Q_{srn} values are below 4 and V_p below 3 km/sec and increase with distance from this zone, reaching about 4.75 km/sec and this indicates an improvement in the Q_{srn} of the rock mass. The result of GL₃₂-GL₇ seismic profiles indicates Q_{srn} is related to the average of V_p (Fig 7). Therefore, it is possible to estimate the average Q_{srn} values by V_p. For mathematical analyses, about 700 datasets were extracted from all raster layers and regression analyses were developed for correlation between Q and Q_{srn} values with V_p. The best fit line of the linear, logarithmic, quadratic, exponential and power equations was selected, and the correlation coefficient (R²) was determined with 95% confidence limits for each regression model (Fig 8). Results show that the best equation between V_p and Q_{srn} (R²=0.69) is more reliable than the best between V_p and Q (R²=0.49). What has changed and improved the performance of the Q_{srn} relative to the Q index is the values of T/V and R_s/S. The definition of these parameters is presented in Table

2. These parameters are well illustrated by the changes in layering properties and rock mass texture. Obviously, these parameters have very influence on the behavior of P-wave velocity in the studied rock masses. In fact, the difference in the relationships presented in Figure 8-a and 8-b relates to the consideration of parameters T/V and R_s/S in Q_{srn}. Since the studied rock masses in this study did not show the phenomenon of karstification and the presence of cavities, the effect of V can be ignored and attributed the correlation increase in figure 8-b to parameters T, R_s and S. As seen in Figure 9, with increasing S, the V_p decreases and it increases with increasing R_s and T. Also, with precision in this figure, it is possible to find out effect of the T/V and R_s/S values on V_p.

3.2. Fuzzy Inference System (FIS)

In the last few years, the fuzzy inference system (FIS) (Lotfzadeh 1965) began to be used in the areas of rock mechanics and engineering geology (e.g., Den-Hartog et al. 1997; Alvarez-Grima and Babuska 1999; Finol et al. 2001; Gokceoglu 2002, etc.). One of the reasons for using FIS in the earth sciences and rock engineering is the high capability of this approach to solving multivariate and nonlinear problems rather than statistical methods. The efficiency of FIS in estimating the mechanical properties of rocks is related to using non-precise and low-relative data to achieve high-relative and relatively precise models so that it has become an efficient and applicable method.

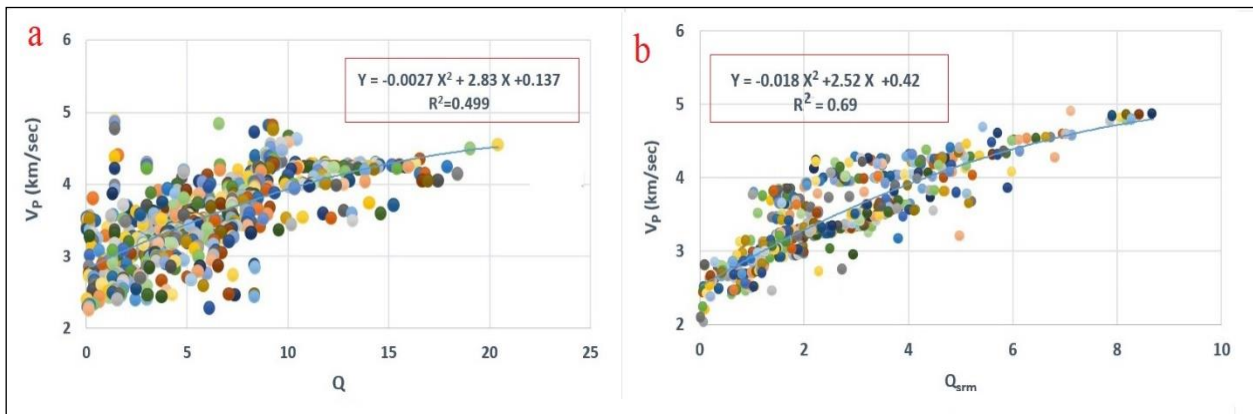


Fig 8. The best fit line and the correlation coefficient (R²) were determined from regression analyses between V_p with Q (a) and Q_{srn}(b)

Table 2. Define values of V, T, Rs, and S in Qsrm (Carrozzo et al. 2008).

T (Texture)	T	V (Void in the rock mass)	V
Homogeneous rock masses	5	A Rock masses without void space	0.5
Sequence of different competent rock types	2	B Rock masses with percentage of void space < 10%	1
Heterogeneous rock masses (sequence of rocks with different features, conglomerates, and breccia.)	0.5	C Rock masses with percentage of void space < 50%	3
Sequence of compact rock types with interbedded clayey layers	0.5	D Rock masses with percentage of void space > 50%	4
		E Softening or low friction clay mineral coatings and small quantities of swelling clays infilling void space of rock mass	5
		F Competent mineral and/or consolidated clay minerals infilling void space of rock mass	2
R _s (Structure)	R _s	S (Bedding)	S
A Massive rock	5	A Horizontal or absent bedding	1
B Metric layers >1m	4	B Inclined (dip direction discordant to rock face dip direction) bedding	0.5
C Decimetric to metric layers >0,5 and <1m	1	C Inclined (dip direction concordant to rock face dip direction) bedding	2
D Decimetric layers <0,5m	0.75	D Inclined (dip direction concordant to rock face dip direction) bedding more than rock face inclination	4
E Laminated	0.5	E Vertical bedding	5

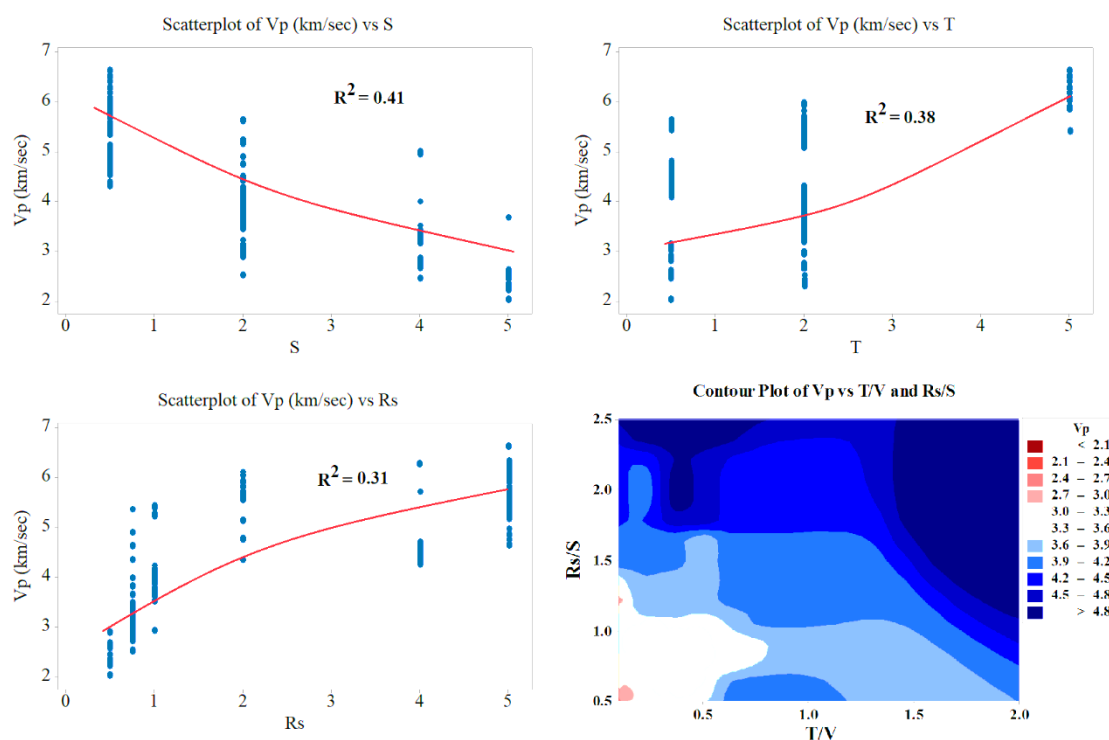


Fig 9. Relationship between T, R_s and S with V_p and contour plot of the relation between V_p with T/V and R_s/S

The high efficiency of FIS has been proven by numerous studies completed on the base of some non-precise data as the input of FIS to reach the valuable and confident outputs (e.g., Fisne et al. 2010; Mosadeghi et al. 2015; Feizi et al. 2017, etc.). In this study, as the previous studies related to the rock engineering (e.g., Kayabasi et al. 2003; Sonmez et al. 2003; Gokceoglu et

al. 2004; Ghasemi et al. 2011; Ghasemi et al. 2012; Jalalifar et al. 2014, etc.), the FIS model based on Takagi-Sugeno (TS) method (Sugeno 1985) was employed to construct a prediction model for the Q_{srm} of Sarvak limestone. The model includes V_p as input and Q_{srm} as the output parameter.

For inference in a rule-based fuzzy model, the fuzzy propositions need to be represented by an implication function called a fuzzy if-then rule or a fuzzy conditional statement (Alvarez-Grima 2000). A fuzzy set is a collection of paired members consisting of members and degrees of confidence for those members. The use of fuzzy sets to present linguistic terms enables one to represent more accurately and consistently something fuzzy (Juang et al., 1992). A linguistic variable whose values are words, phrases or sentences are labels of fuzzy sets (Lotfizadeh 1973). In literature, many methods such as intuition, rank ordering, angular fuzzy sets, genetic algorithms, inductive reasoning, soft partitioning, etc. exist for the membership value assignment (e.g., Lotfizadeh 1972; Hadipriono and Sun 1990; Karr and Gentry 1993). Traditionally, a fuzzy model is built by using expert knowledge in the form of linguistic rules, and there is an increasing interest in obtaining fuzzy models from measured data (Setnes et al. 1998).

In this study, fuzzy sets of membership functions (MF) were extracted from the relationships between inputs and outputs, because they are sufficiently accurate and the number of data (700 datasets) is sufficient to extract the sets. The graphical illustrations of the membership function are given in Figure 10 (completed by MATLAB.8 software).

This study aimed mainly to construct the rule-based TS fuzzy inference system in which the relations between the different variables were represented using fuzzy implications or fuzzy if-then rules of the form: If antecedent then consequent. To convert non-fuzzy sets to fuzzy, specific functions known as MF were employed. Here, the MFes of FIS designed were one

order (linear) functions, which could be presented in the form of an $m \times n$ matrix; where m is the number of rows and n is the number of columns. Every row in this matrix indicated factors of a particular output MF. In every FIS, to create a logical relation among inputs and outputs, several conditional rules are required (Gustafson and Kessel 1978). To obtain optimal fuzzy models, data were divided into several categories based on the wave velocity (Table 3). Several fuzzy models were evaluated on the categories of data. The results showed that for samples with a $V_p < 3.5$ km/sec (very low and low velocity) and $V_p > 3.5$ km/sec (moderate and high velocity), different fuzzy functions can be obtained. In this case, for the FIS to estimate Q_{srm} , 26 rules (14 rules for $V_p < 3.5$ km/sec and 12 rules for $V_p > 3.5$ km/sec) were built and two distinctive FIS models were presented to estimating of Q_{srm} (Fig 10). In Figure 10, every MF represents the range of changes in the Q_{srm} index for the variations in the V_p . Gaussian MF (Equation 2) was used through a Gaussian or normal distribution based on an intermediate point with the degree of membership 1. To obtain each MF, the authors used equations whose constant coefficients are shown in the matrix of each model.

Also, the degree of membership (0-1) of each function represents the degree of effectiveness of each equation by the variation of the V_p . The models reached minimum error after 25 training steps for $V_p < 3.5$ km/sec and after 18 training steps for $V_p > 3.5$ km/sec (Fig 11).

$$\mu(x) = e^{-f1*(x-f2)^2} \tag{2}$$

The inputs of equation 4 are $f1$ and $f2$ that were the spread and the midpoint, respectively.

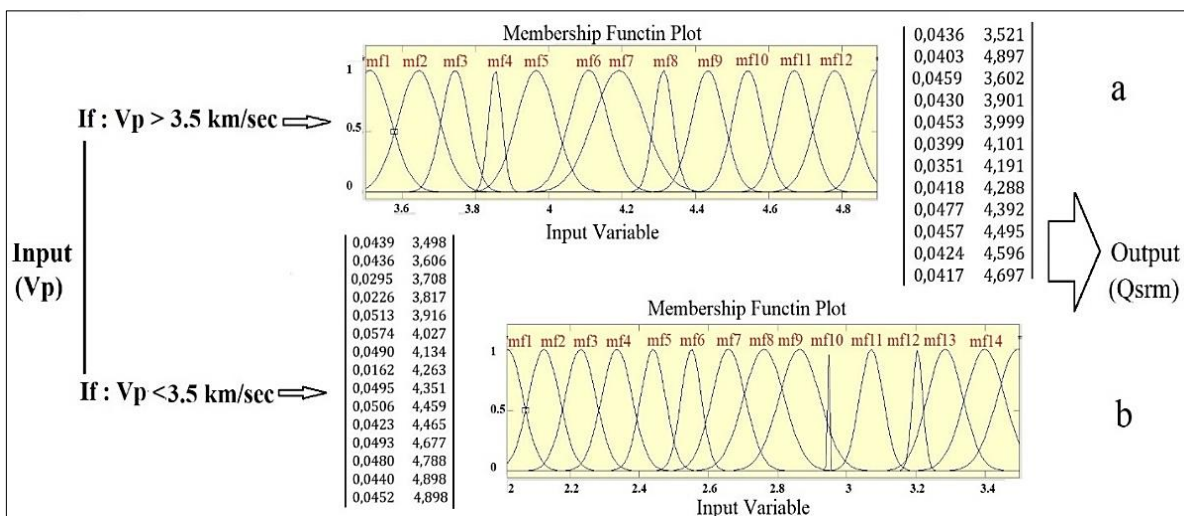


Fig 10. FIS models and the matrix of parameters are presented for estimating of Q_{srm} for data sets by $V_p > 3.5$ km/sec (a) and $V_p < 3.5$ km/sec (b).

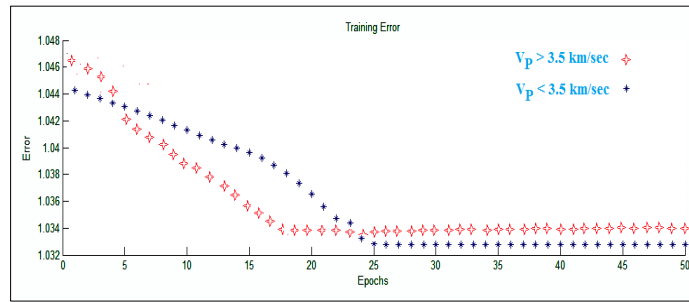


Fig 11. Training steps, models reached its minimum error.

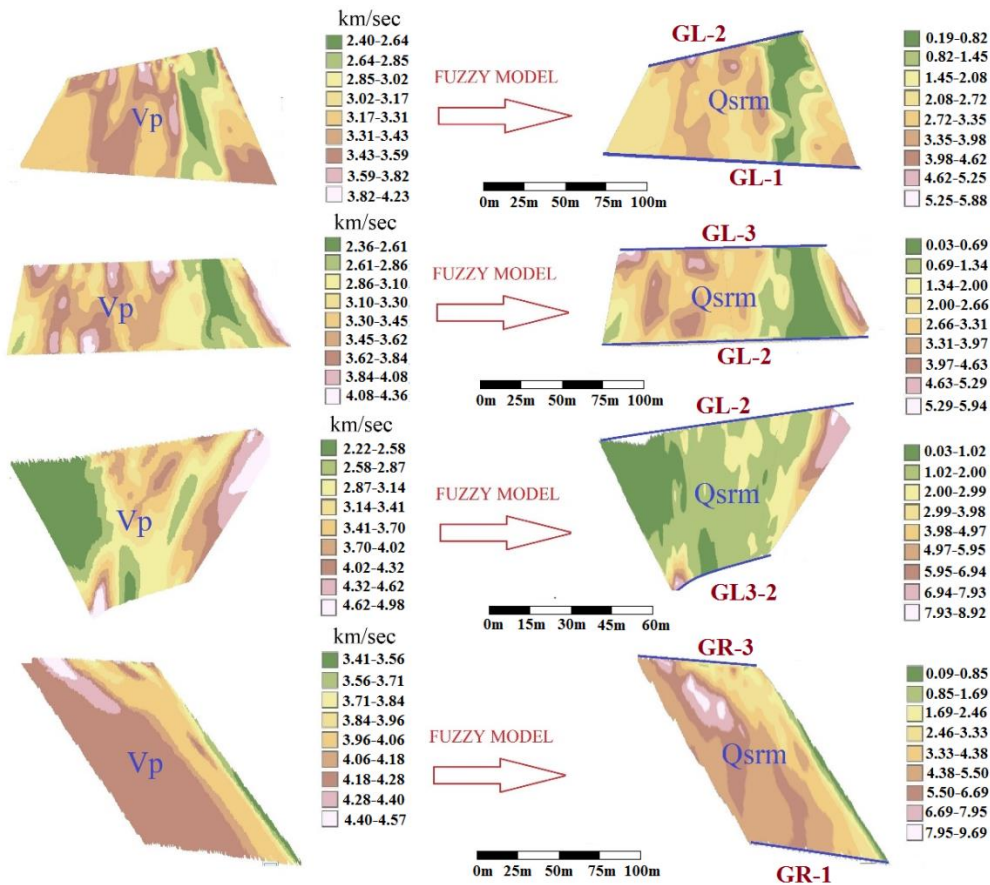


Fig 12. Raster layers that created by interpolation of V_p values and predicted Q_{srm} by FIS models (Data-sets used for training of models).

The last stage of a FIS is the defuzzification stage. Therefore, input data were converted to fuzzy sets using the membership functions presented in Figure 10. As shown in Figure 10 and according to the rules designed by the logic operator (prod function), the input parameter turned into Z_i function and degree of infection (W_{ii}) using Equations 3 and 4, respectively.

$$Z_i = a_i x_i + k_i \quad (3)$$

Where a and k are parameters presented as every row in matrixes of Figure 10. It means that x_i is V_p for each section. Equation 2 was applied to make the output defuzzy and to gain value of Z , which is the answer to the model (Equation 3).

$$Z = \sum_{i=1}^n Z_i \left(\frac{W_{ii}}{\sum W_{ii}} \right) \quad (4)$$

Where n is the number of rules, W_{ii} is the degree of infection derived from the operation of the method (prod function) on the membership functions in each rule, and Z_i is from Equation 3.

4. Discussion and results

After the defuzzification stage, all Q_{srm} indices, predicted by FIS models, were turned into three-dimensional raster layers in ArcGIS 10.3.1 software package. Figure 12, show raster layers of Q_{srm} indexes, predicted by FIS models of V_p .

Table 3. Defined ranges for V_p (Anon 1979)

Range of V_p	Very Low	Low	Moderate	High	Very High
	<2.5	2.5-3.5	3.5-4	4-5	>5
Number of data	107	165	283	124	0

As shown in this figure, FIS models have a good prediction of Q_{srm} . By extract multi-values to points from all raster layers, regression analyses were developed for FIS Q_{srm} recorded values with V_p . The cross-correlation between predicted and measured data was applied (Fig 13), and the strong coefficient of determination was calculated as 0.83.

For checking the in-situ performance and testing of the designed FIS models, another tomography section of BDS was selected. Therefore, predicted in-situ values by FIS model, after the defuzzification and interpolation, were turned into three-dimensional raster layers in ArcGIS. Figure 14, show raster layers of V_p (input value) and Q_{srm} indexes predicted by the FIS model.

Relations between Q_{srm} resulted from FIS models and in-situ measuring, are shown in Figure 15. This relation has a determination coefficient (R^2) of 0.81. Obviously, in this section, the predictive capability of the FIS model, for prediction of Q_{srm} , is significant. Figures 13

and 15 show a good correlation between predicted and measured Q_{srm} values with a coefficient of determination of 0.83 and 0.81, respectively. Also, the variance account for (VAF) (Equation 5) and the root mean square error (RMSE) (Equation 6) indices were also employed to control the performance of the prediction capacity of the FIS as utilized by Alvarez-Grima and Babuska (1999).

$$VAF = (1 - \frac{\text{var}(y - y')}{\text{var}(y)}) \times 100 \tag{5}$$

$$RMSE = \sqrt{\frac{1}{N} \sum_{i=1}^N (y - y')^2} \tag{6}$$

Where, y and y' are data measured in situ and predicted values by statistical or FIS techniques, respectively. The calculated indices for regression and FIS models for prediction of Q and Q_{srm} are given in Table 4. The models will be excellent, provided that the VAF is 100 and RMSE is 0. Therefore, FIS models for prediction of Q_{srm} are the best.

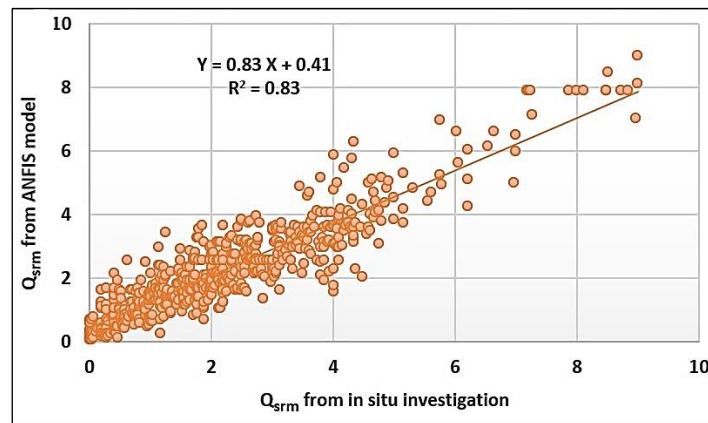


Fig 13. The relation between predicted Q_{srm} by the FIS models and measured in-situ values.

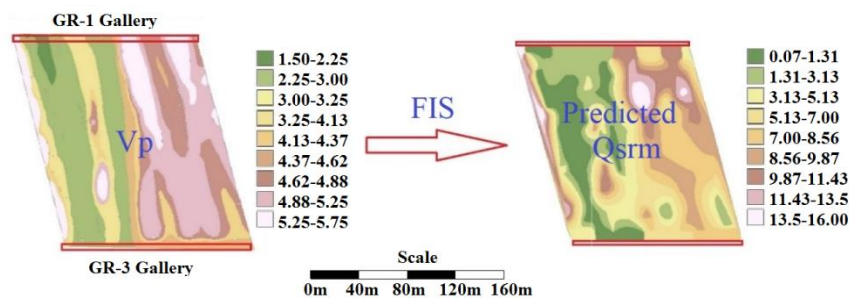


Fig 14. Raster layer that created by interpolation of V_p values and predicted Q_{srm} by FIS models (Data-sets used for testing of models).

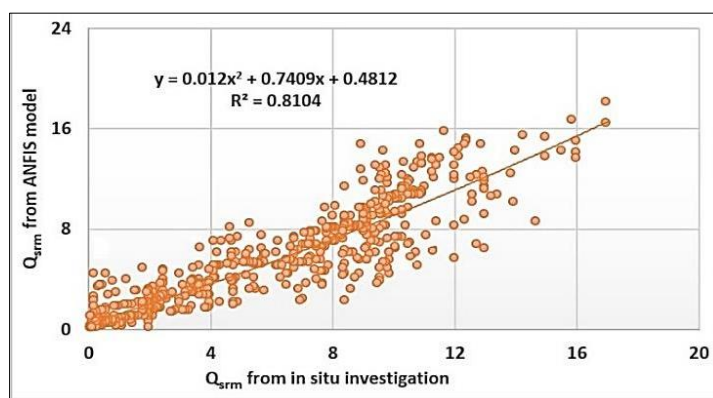


Fig 15. The relation between predicted FIS values and measured in-situ Q_{srm} values (Datasets used for testing of models).

Table 4-Values of VAF and RMSE computed for the designed models

Model	Predicted parameter	R^2	VAF (%)	RMSE
Best regression	Q	0.499	30.583	37.856
Best regression	Q_{srm}	0.691	94.886	8.943
FIS	Q_{srm}	0.823	95.661	7.933

5. Conclusions

Many attempts have been made to correlate V_p with the mechanical properties of Sarvak formation limestone for the initial assessment of the rock-mass quality. This study had shown acceptable correlations between rock quality classifications (Q and Q_{srm}) and a seismic rock classification based on V_p . The seismic data obtained at the BDS in SW Iran. Q_{srm} classification system ranks the various units of limestone rock mass of BDS as very poor to the fair where the Q system ranks it as very poor to good. The relationship between the V_p with Q and Q_{srm} showed medium (0.49) and good (0.69) coefficients of determinations. Also, by FIS models for prediction of Q_{srm} , its correlation coefficient increases to 0.83.

It seemed that the correlation between the V_p and the Q_{srm} classification system is more reliable because this system takes into consideration more parameters of rock mass such as dipping of the layers, bedding, cavities, and texture. In fact, with increasing values of T and R_s , the V_p increases and with the increase of S, the V_p decreases. This shows the effect of layering and rock mass changes in Q_{srm} classification. Also, comparing the values of R^2 , VAF and RMSE of resulted equations from regression analyses and FIS techniques, showed that resulted from approaches using the FIS technique to predict Q_{srm} are very more reliable than statistical methods. Therefore, in the studied area, the predictive performance of V_p and FIS models, for prediction of Q_{srm} , is significant. It is suggested that the models obtained in this study could be applied to areas that have similar lithological and structural characteristics to the studied area but cannot be extended to other rock types.

Acknowledgments

The authors would like to thank the managers of Mahab Ghodss Consulting Engineers and also the authorities of the Bakhtiari Dam project for helping to carry out data and the geotechnical and geophysical field works. We also wish to thank anonymous reviewers for insightful comments that helped improve the quality of the manuscript.

References

- Alvarez-Grima M, Babuska R (1999) Fuzzy model for the prediction of unconfined compressive strength of rock samples. *International Journal of Rock Mechanics and Mining* 36: 339–349
- Alvarez-Grima M (2000) Neuro-fuzzy modeling in Engineering Geology. A.A. Balkema, Rotterdam, 244pp.
- Juang, C.H., Lee, D.H., Sheu, C., 1992. *Mapping slope failure potential using fuzzy sets*, *Journal of Geotechnical Engineering ASCE* 118 (3): 475–493.
- Anon (1979) Classification of rocks and soils for engineering geological mapping, *Bulletin of the International Association of Engineering Geology* 5: 89–112.
- Azwini N, Saad R, Saidin M, Nordiana MM, Bery AA, Hidayah IN (2015) Combined analysis of 2-D electrical resistivity, seismic refraction and geotechnical investigations for Bukit Bunuh complex crater IOP Conference Series: *Earth and Environmental Science* 23(1):12-13.
- Barton N, Lien R, Lunde, J (1974) Engineering classification of rock masses for the design of tunnel support, *Journal Rock Mechanics Engineering* 6: 189–236.

- Barton N (1991) Geotechnical design, *World Tunnelling*, pp:410–416.
- Barton N (1995) The influence of joint properties in modelling jointed rock masses, Proc. Int. ISRM Congr. on Rock Mech, Tokyo, Japan, T. Fujii ed., A.A. Balkema: Rotterdam, pp:1023–1032.
- Barton N (2002) Some new Q-value correlations to assist in site characterization and tunnel design, *International Journal of Rock Mechanics and Mining Sciences* 39:185–216.
- Barton N (2007) Future directions for rock mass classification and characterization – Towards a cross-disciplinary approach, Oslo, Norway.
- Barton N (2008) Bakhtiari Dam & HPP: First site visit report by N.B&A (in Persian).
- Bery A, Saad R (2012) Correlation of seismic P-wave velocities with engineering parameters (N value and rock quality) for tropical environmental study, *International Journal of Geosciences* 3(4): 749-757.
- Bery AA, Rosli S (2012) Correlation of Seismic P-Wave Velocities with Engineering Parameters (N Value and Rock Quality) for Tropical Environmental Study. *International Journal of Geoscience* 3: 749-757.
- Bieniawski ZT (1973) Engineering classification of jointed rock masses, *Trans S. Afr. Inst. Civil Engineer in South Africa* 15:335-344.
- Cardarelli E, Marrone C, Orlando L (2006) Evaluation of tunnel stability using integrated geophysical methods. *Journal of Applied Geophysics* 52: 93-102.
- Carrozzo MT, Leucci G, Margiotta S, Mazzone F, Negri S (2008) Integrated geophysical and geological investigations applied to sedimentary rock mass characterization, Lecce, Italy, university of Salento, *Department of Science and Material. Annals of Geophysics* 51(1): 191-202.
- Cheng J, Li L, Yu S, Song Y, Wen Xinglin (2001) Assessing changes in the mechanical condition of rock masses using P-wave computerized tomography, *International Journal of Rock Mechanics and Mining Sciences* 38: 1065–1070.
- Deere DU (1963) Technical Description of Rock Cores for Engineering Purposes, rock mechanic and engineering geology, *Journal of Rock Mechanics and Engineering Geology* 1:16-22.
- Den-Hartog MH, Babuska R, Deketh HJR, Alvarez Grima M, Verhoef PNW, Verbruggen HB (1997) Knowledge-based fuzzy model for performance prediction of a rock-cutting trencher, *International Journal of Approximate Reasoning* 16:43-66.
- Fan LF, Wang LJ, Wu ZJ (2018) Wave transmission across linearly jointed complex rock masses. *International Journal of Rock Mechanics and Mining Sciences* 112: 193-200.
- Feizi F, Ramezani AK, Mansouri E (2017) Calcic iron skarn prospectively mapping based on fuzzy AHP method, a case study in Varan area, Markazi province, *Journal of Geoscience* 21: 123-126.
- Finol J, Guo YK, Jing XD (2001) A rule based fuzzy model for the prediction of petro physical rock parameters, *Journal of Petroleum Science and Engineering* 29(2):97–113.
- Fisne A, Kuzu C, Hudaverdi T (2010) Prediction of environmental impacts of quarry blasting operation using fuzzy logic, *Environmental Monitoring and Assessment. Epub ahead of print.* doi: 10.1007/s10661-010-1470-z.
- Cha YH, Kang JS, Jo CH (2006) Application of linear-array microtremor surveys for rock mass classification in urban tunnel design, *Exploration Geophysics* 37 (1): 108-113.
- Cao A, Dou L, Cai W, Gong S, Liu S, Jing G (2015) Case study of seismic hazard assessment in underground coal mining using passive tomography. *International Journal of Rock Mechanics and Mining Sciences* 78: 1-9.
- Ghasemi E, Ataei M, Hashemolhosseini H (2012) Development of a fuzzy model for predicting ground vibration caused by rock blasting in surface mining, *Journal of Vibration and Control.* doi: 10.1177/1077546312437002.
- Ghasemi E, Ataei M, Shahriar K (2011) Prediction of roof fall rate in coal mines using fuzzy logic, *Proceedings of the 30th International Conference on Ground Control in Mining, University of West Virginia, Morgantown, WV*, 186-191.
- Gokceoglu C (2002) A fuzzy triangular chart to predict the uniaxial compressive strength of Ankara agglomerates from their petrographic composition, *Engineering Geology* 66: 39–51.
- Gokceoglu C, Yesilnacar E, Sonmez, H, Kayabasi A (2004) A neuro-fuzzy model for modulus of deformation of jointed rock masses, *Journal of Computers and Geotechnics* 31(5):375–383.
- Grima MA Babuska R (1999) Fuzzy model for the prediction of unconfined compressive strength of rock samples, *International Journal of Rock Mechanics and Mining Sciences* 36(3):339–349.
- Gustafson D, Kessel W (1978) Fuzzy clustering with a fuzzy covariance matrix, In 1978 IEEE conference on decision and control including the 17th symposium on adaptive processes 17:761–766.
- Hadipriono F, Sun, K (1990) Angular fuzzy set models for linguistic values, *Civil Engineering Systems* 7 (3):148–156.
- Hemmati-Nourani M, Taheri Moghadder M, Safari M (2017) Classification and assessment of rock mass parameters in Choghart iron mine using P-wave velocity, *Journal of Rock Mechanics and Geotechnics Engineering* 9:318–328.
- Hoek E (1994) Strength of rock and rock masses, *ISRM News Journal* 2(2):4-16.
- Hoek E, Kaiser PK, Bawden WF (1995) Support of underground excavations in hard rock Rotterdam: Balkema.

- Hoek E, Brown ET (1997) Practical estimates of rock mass strength, *International Journal of Rock Mechanics and Mining* 34(8):1165–86.
- Iran Water and Power Resourced Development Co, (2007). "Final Report of Rock Mechanics of Bakhtiari Dam (in Persian).
- Iran Water and Power Resourced Development Co (2008). Geological Report of Bakhtiyari Dam (in Persian).
- Jalalifar H, Mojedifar S, Sahebi AA (2014) Prediction of rock mass rating using fuzzy logic and multi-variable regression model, *International Journal of Mining Science and Technology* 24:237–2.
- Karr CL, Gentry EJ (1993) Fuzzy control of pH using genetic algorithms, *IEEE Transaction on Fuzzy Systems* 1 (1):46–53.
- Kayabasi A, Gokceoglu C, Ercanoglu E (2003) Estimating the deformation modulus of rock masses: a comparative study, *International Journal of Rock Mechanics and Mining Sciences* 40: 55–63.
- Krau F, Giese R, Alexandrakis C, Buske S (2014) Seismic travel-time and attenuation tomography to characterize the excavation damaged zone and the surrounding rock mass of a newly excavated ramp and chamber. *International Journal of Rock Mechanics and Mining Sciences* 70: 524-532.
- Leucci G, Giorgi LD (2006) Experimental studies on the effects of fracture on the P and S wave velocity propagation in sedimentary rock (Calcarenite del Salento), *Journal of Engineering Geology* 84 (3-4):130-142.
- Leucci G, Giorgi LD (2015) 2D and 3D seismic measurements to evaluate the collapse risk of an important prehistoric cave in soft carbonate rock; *Open Geosci* 84–94.
- Lotfizadeh LA (1965) Fuzzy sets, *Information and Control* 8 (3): 338–353.
- Lotfizadeh LA (1972) A rationale for fuzzy control. *Journal of Dynamic Systems, Measurement and Control Transaction, ASME* 94: 3-4.
- Lotfizadeh LA (1973) Outline of a new approach to the analysis of complex systems and decision processes, *IEEE Transactions on Systems Man and Cybernetics* 3:28–44.
- Marinos P, Hoek E (2001) Estimating the geotechnical properties of heterogeneous rock masses such as flysch, *Bulletin of the Engineering Geology & the Environment* 60: 85-92.
- Mosadeghi R, Warnken J, Tomlinson R, Mirfenderesk H (2015) Comparison of Fuzzy-AHP and AHP in a spatial multi-criteria decision-making model for urban land-use planning, *Journal of Computers Environment and urban systems* 49:54-65.
- Sabir Co (2004) Geophysical survey of Bakhtiari dam and power site by using seismic refraction and tomography (in Persian).
- Setnes M, Babuska R, Verbruggen HB (1998) Rule-based modeling: precision and transparency, *IEEE Transactions on Systems Man and Cybernetics*, Part C 28:165–169.
- Sonmez H, Gokceoglu C, UlusayR (2003) an application of fuzzy sets to the Geological Strength Index (GSI) system used in rock engineering, *Engineering Applications of Artificial Intelligence* 16: 251–269.
- Sugeno M (1985) Industrial applications of fuzzy control, New York, USA. *Elsevier Science Pub. Co* 269 pp.
- Telford WM, Geldart LP, Sheriff RE (1990) Applied geophysics, *Cambridge University Press, Cambridge, UK*.
- Vilhelm J, Ivankina T, Lokajiček T, Rudajev V (2016) Comparison of laboratory and field measurements of P and S wave velocities of a peridotite rock. *International Journal of Rock Mechanics and Mining Sciences*. 88: 235-241.
- Zafirovski Z, Peševsk I, Papić J (2012) Methodology for extrapolation of rock mass deformability parameters in tunneling, *Facta Universitatis Series: Architecture and Civil Engineering* 10 (3): 235-244.